ERJ Express. Published on February 27, 2009 as doi: 10.1183/09031936.00101008

Local effector failure in mesothelioma is not mediated by $CD4^+CD25^+$Treg cells

Authors: Connie Jackaman[§], Scott Cornwall[#∞], Andrew M. Lew[‡], Yifan Zhan[‡], Bruce W.S. Robinson[§] and Delia J. Nelson[#§∞].

Note that Connie Jackaman and Scott Cornwall contributed equally to this work.

[#]Curtin University, School of Biomedical Sciences, Bentley, Perth, Western Australia, Australia, 6102; [§]University of Western Australia, School of Medicine and Pharmacology, Perth, Western Australia, Australia, 6009; [‡]Walter and Eliza Hall Institute, Melbourne, Victoria, Australia 3050; [∞]Western Australia Biomedical Research Institute, Bentley, Perth.

Address correspondence to Dr Delia Nelson, Curtin University, School of Biomedical Sciences, Kent St., Bentley, Western Australia, Australia, 6102.
Tel: 618 9361 9058; Fax: 618 93612027 ; E-mail: DeliaNelson@curtin.edu.au

Short title: Treg depletion may not help mesothelioma patients

Abstract

Aims: To define the point at which mesothelioma T cell responses fail in order to design better immunotherapies. **Approach**: We used a murine model of mesothelioma that was established with asbestos, and inoculation of tumor cells into syngeneic mice results in progressing tumors with similar histopathology to human mesothelioma. The tumor cells secrete a marker tumor antigen similar to secreted tumor-associated products such as mesothelin. **Results**: The mesothelioma microenvironment contains stromal elements including dendritic cells, effector $CD8^+$ and $CD4^+$ T cells, and $CD4^+$ T regulatory cells (Tregs), all of which are activated in situ, implying chronic inflammation. Tumor antigens are rapidly transported to draining lymph nodes wherein tumor-specific T cell responses are generated. Despite the generation of potent $CD8^+$ CTL in lymphoid organs, those that infiltrate tumors cannot restrain tumor growth suggesting local suppression. Splenic Tregs did not suppress protective responses in adoptive transfer experiments suggesting that systemic Treg play little role in regulating anti-mesothelioma immune responses. Finally removal of $CD25^+$ Tregs from the tumor site and lymphoid organs did not alter tumor growth with or without IL-2 or IL-21 immunotherapy. **Conclusions**: Treg cells are not potent regulators of anti-mesothelioma immunity and targeting these cells may not improve results.

Introduction

Malignant mesothelioma (MM) is caused by exposure to asbestos fibres. Although its period of development spans decades, its clinical course upon detection is generally rapid and fatal. As the incidence of this disease is predicted to rise (1) and MM is resistant to most current treatment modalities there is a pressing need for new therapeutic approaches. The occasional spontaneous regression in humans (2), and partial responses to immunotherapeutic agents that do not involve external sources of tumor antigen in clinical trials (3-7) support the notion that the immune system can recognise MM. Thus, MM may be similar to other immunogenic cancers in which anti-tumor T-cell responses can been detected in patients' peripheral blood and tumors in the absence of treatment (8-11). In order to improve MM immunotherapy it is essential that we understand where the immune system fails to respond to the tumor. A murine model of MM has shown that the immune system is not ignorant of this disease (12, 13), however, these studies focussed only on events in occurring in secondary lymphoid organs. In this study we also examine the status of anti-MM T-cells at the effector site, the tumor itself.

Rational strategies for immune intervention will require an understanding of the relationship between the immune system and MM microenvironment. Effector T cells may be rendered dysfunctional via local immunosuppressive mechanisms (14-17) such as T-cell anergy due to insufficient costimulation and suppression by regulatory cells or soluble factors. Such mechanisms have been described in MM (17-19). Yet, when immunotherapy is applied directly into the tumor bed the anti-MM immune response is often augmented in animal models (20-23), and in clinical trials (7, 24-27). These data suggest that the MM microenvironment limits T-cell responses but can be conditioned to support a powerful effector arm.

The murine MM cell line, AE17, was developed by injecting asbestos fibres into the peritoneal cavity of C57BL/6J mice. The histopathology of tumors arising from subcutaneously injected AE17 MM cells is very similar to that of human MM (23). However, the lack of a known MM-specific tumor antigen has hindered in-depth studies of adaptive immune responses to MM, and the only other murine model used to date expresses a membrane-bound, influenza antigen as a model antigen (13). Recent studies have shown

that secreted proteins such as soluble mesothelin-related proteins (SMRP) may be a useful diagnostic and prognostic mesothelioma-specific antigen (28, 29). The AE17 MM cell line was transfected with secreted ovalbumin (AE17-sOVA) (23) such that OVA becomes a 'marker' tumor antigen to which immune responses can be monitored.

Our aim was to identify the point at which mesothelioma immune responses to a secreted-MM antigen fail by characterizing the anti-mesothelioma T cell response. We first confirmed the presence of tumor-infiltrating dendritic cells (DC) as they have capacity to take up tumor antigens within the MM tumor microenvironment. We then assessed if, and when, our spy tumor antigen was presented to T cells in tumor draining lymph nodes (dLN), and whether the tumor-specific $CD8^+$ CTL that were generated penetrated the tumor microenvironment. Finally, tumor-infiltrating effector $CD8^+$ and $CD4^+$ T cells, as well regulatory $CD4^+$ T cells were examined for evidence of local activation and function during untreated progression, as well as during IL-2 or IL-21 immunotherapy.

Materials and methods

Mice

Female C57Bl/6J (H-2^b) mice aged 6-8 weeks were obtained from the Animal Resources Centre (Western Australia) and maintained under standard housing conditions. The TCR transgenic mouse line, OT-1, expressing a TCR recognizing the H-$2K^b$ restricted dominant $OVA_{257-264}$ peptide SIINFEKL (OVAp) (30), was kindly supplied by Dr. F Carbone and Dr. W. Heath (University of Melbourne, Australia). GK mice are transgenic for the depleting anti-CD4 Ab, GK1.5, and so have no peripheral CD4 T cells (31). GK and perforin$^{-/-}$ mice (32) were bred and housed at the Walter and Eliza Hall Institute (WEHI).

Murine mesothelioma tumor cell line, tumor induction and in vivo growth

AE17 is a MM cell line derived from the peritoneal cavity of C57BL/6J mice injected with asbestos fibres; both AE17 and its OVA transfectant, AE17sOVA have been previously described (23). On day 0, mice were injected subcutaneously (s.c.) into the right hind flank with $5x10^5$ tumor cells in 100µl of PBS, and the rate of tumor growth measured (mm^2) using micro-callipers. All procedures were performed with approval by the University of Western Australia, Curtin University and WEHI Animal Experimentation Ethics Committees' (AEC) approval conditions. In general, the AECs only permitted tumor growth up to $100mm^2$ however, the Curtin University AEC gave conditional short-term approval for an endpoint of $150mm^2$ so that treatment efficacies could be assessed in greater depth.

Harvesting tissues

Tissues were removed and either embedded in OCT and immediately cryopreserved for immunohistochemistry, or prepared as single cell suspensions by mashing gently between two frosted glass slides in PBS/2%FCS.

In vivo analysis of antigen presentation (Lyons-Parish assay)

5,6-carboxy-fluorescein-succinimidyl-ester (CFSE; Molecular Probes, Eugene, OR) labeling was performed as previously described (33). LN cells from TCR transgenic OT-1 mice were incubated with CFSE (5mM in DMSO) for 10min at room

temperature. Cells were washed and 10^7 cells i.v. injected into each recipient mouse. CFSE-labeled cells were analyzed by FACS analysis 3 days post adoptive transfer.

In vivo analysis of CTL function ('in vivo CTL assay')

Target cells for *in vivo* evaluation of cytotoxic activity were prepared as we have described elsewhere (23). Briefly, C57BL/6 LN cell suspensions were RBC-lysed, washed and divided into two populations. One population was pulsed with 10^{-6}M OVAp for 90min at 37°C, washed in PBS and labeled with a high concentration (5μM) of CFSE. Control, uncoated target cells were labeled with a low concentration of CFSE (0.5μM). 10^7 cells of each population were mixed in 200μl PBS and i.v. injected into each recipient mouse. Specific *in vivo* cytotoxicity was determined by collecting the relevant organs from recipient mice 18h post injection and the number of cells in each target cell population determined by flow cytometry. The ratio between the percentages of uncoated versus OVAp-coated ($CFSE^{Lo}/CFSE^{high}$) was calculated to obtain a numerical value of cytotoxicity. To normalize data allowing inter-experimental comparisons, ratios were calculated between the percentages of peptide coated in control versus tumor-bearing mice.

FACS analysis

Single cell suspensions were stained with a combination of; CD4 (RM 4-5), CD8α (53-6.7), CD11c (HC3), CD45R/B220 (RA3-6B2), anti-murine IFNγ, CD62L (MEL-14), CD69 (H1.2F3), CD44 (IM7), CD25 (3C7) (all from Pharmingen), F4/80 (clone CI:A3-1; Caltag) CD4 (RM 4-5) (eBioscience), CD25 (PC61), FoxP3 (150D) (Biolegend) and/or PE-labelled OVAp-H-$2K^b$ tetramer (kindly provided by Dr. Andrew Brooks, Uni. of Melbourne; Victoria). Analysis was performed on a FACScan (Becton Dickinson, Mountain View, CA) using CellQuest and FlowJo software or on a FACSCanto II using FACSDiva software.

Immunohistochemistry

Frozen sections were fixed in cold ethanol. Endogenous peroxidases, avidin and biotin were blocked using 1% hydrogen peroxide and the Avidin/Biotin blocking kit (Dako). For single staining primary Abs directed against murine CD4 and CD8, CD11c, B220 (clone RA3-6B2, Pharmingen), F4/80, CD31 (clone MEC 13.3; Pharmingen) and isotype controls (rat

$IgG2_a$, rat $IgG2_b$, and hamster IgG) were consecutively linked to a secondary biotinylated Ab (anti-rat mAb; Jackson ImmunoResearch, West Grove, PA), or anti-hamster Ab (PharMingen), followed by streptavidin-HRP (Dako, Glostrup, Denmark). After washing, one Sigma FAST™ (D-4168) DAB (3,3-Diaminobenzidine) tablet and one urea hydrogen tablet (Sigma, St. Louis, MO) were added to ddH_2O to serve as a peroxidase substrate (125µl/section) and hematoxylin counterstained to visualize staining. Sections were then dehydrated and mounted with DPX (Ultramount, Scot Scientific).

For double staining, primary Abs were linked to a peroxidase-conjugated antibody (rabbit anti-rat or anti-hamster; Dako Denmark) and detected using DAB substrate as a peroxidase substrate. A biotinylated primary antibody linked to streptavidin-alkaline phosphate (SA-AP; DAKO) was visualised using an alkaline phosphatase substrate (BCIP/NBT; Vector). Sections were mounted in Immunomount (Shandon, Pittsburgh, PA).

In vivo depletion using monoclonal antibodies

For depletion of $CD4^+$ or $CD8^+$ cells, 2 doses (150µg/dose) of either YTS-191 or YTS-169 (European Collection of Animal Cell Cultures; Salisbury, UK) respectively were injected i.p. with 3 doses/week (100-150µg/dose) for two weeks and spleens tested (by FACS analysis); $CD8^+$ depletions were 95-99% effective, whilst $CD4^+$ depletions were 90-95% effective (data not shown). For depletion of $CD25^+$ cells, 1 or 2 doses (150µg/dose) of PC61 (anti-mouse CD25 monoclonal antibody obtained from the Monoclonal Antibody Facility; Perth, Western Australia) in 100µl PBS were injected intra-tumorally or peri-tumorally (34). The endotoxin levels in PC61 was < 0.1 EU/ml (measured by supplier using an endotoxin detection kit, documentation supplied).

IL-2 and IL-21 immunotherapy

Lyophilized Proleukin (recombinant IL-2; Cetus Corporation, Emeryville, CA, USA) was reconstituted in sterile PBS (Sigma) and given intratumorally as previously described (23). The vector pORF.mIL-21 (Invivogen, San Diego, CA, USA) was used for the production of IL-21 in-vivo; 20µg of plasmid in 2ml of saline was injected hydrodynamically (35).

Statistical analysis

Statistical significance was calculated using GraphPad (San Diego, CA) PRISM. Student's *t* test was used to determine differences between two populations. One-way ANOVA was used to determine differences between more than two populations.

Results

DC are located in the mesothelioma tumor microenvironment

DCs are highly efficient at capturing and processing in situ antigen for presentation to T cell after trafficking to draining lymph nodes (dLN). Thus, tumor-infiltrating DC represent a likely candidate for priming the anti-tumor response. Therefore, the first series of studies examined tumor-infiltrating DC in progressing tumors that were divided into previously defined MM tumor sizes based upon their responsiveness to IL-2 immunotherapy; i.e. tumors less than $25mm^2$ are readily cured after intratumoral (i.t.) IL-2 treatment, whilst 100% of those greater than $25mm^2$ completely fail to respond (23). Therefore, small tumors are defined as those < $25mm^2$, medium sized tumors are between $25mm^2$ and $50mm^2$, and large tumors are 50-$100mm^2$. Note that in accordance with AEC conditions we are unable to grow tumors beyond $100mm^2$. Tumors were sampled when they were small (< $25mm^2$) versus 'medium' sized (between $25mm^2$ and $50mm^2$).

CD11c is a pan DC marker and $CD11c^+$ cells were found infiltrating tumors (Fig. 1A) and their proportional abundance did not significantly alter during tumor progression. Interestingly, the percent of $CD11c^+$ DC in dLN in animals bearing medium tumors was significantly higher than DC levels seen in normal LN controls (Fig 1A).

MM tumor antigens are rapidly transported to dLN for presentation to T cells

One possible role of tumor-residing DC is the presentation of tumor antigens to naïve T cells in dLN. Therefore, we assessed whether tumor antigens are presented *in vivo* in LN during disease progression using the AE17-sOVA cell line. AE17sOVA is readily recognized by OVA-specific CTL taken from OT-I mice (23) therefore antigen presentation was identified by OT-I $CD8^+$ T cell proliferation in vivo. To do this CFSE-labelled OT-I cells were intravenously injected into tumor-bearing mice previously given tumor cells. After 3 days, lymphoid organs were collected and OT-I proliferation assessed by CFSE dilution.

As expected, antigen presentation was primarily seen in the dLN (Fig 1B). Unlike other MM models wherein tumor antigen presentation was restricted to the dLN (13), some limited proliferation was seen in non-dLN (Fig 1C), presumably because OVA was

secreted. Antigen presentation could be detected even when tumors were small. These results show that tumor antigen presentation occurs early in MM tumor growth.

Tumor-specific CTL are initially generated in draining LN and spread systemically

We next assessed whether the antigen presentation seen above led to the generation of tumor-specific CTL in LN. OVAp-pulsed CFSE-labelled target cells were adoptively transferred into AE17sOVA tumor-bearing mice, and lymphoid organs analyzed by FACS 18hrs later. OVAp-specific CTL in dLN could be detected in mice with small tumors and their killing activity significantly increased with increased tumor burden (Fig 1J). Note that as tumor burden increased OVAp-specific CTL were also found at equivalent levels in non-draining LN implying systemic spread of these CTL (Fig 1F, G and J). These results show that tumor antigen presentation and the generation of tumor-specific CTL occurs early in MM tumor growth.

Small numbers of $CD8^+$ T cells infiltrate MM tumors

Next we wanted to address whether the T cells generated in the dLN migrated into the MM tumor microenvironment. Initially, this was assessed using FACS analysis (Fig.2A) of tumors disaggregated to single cells and immunohistochemistry on frozen tumor sections (data not shown); both were stained with anti-CD8 antibodies. Small percentages (3.4% to 5.2%) of $CD8^+$ cells were present within MM tumors (Fig. 2A). Interestingly, the percentage of $CD8^+$ cells within LN increased in small tumor-bearing mice but fell to normal levels as MM tumors progressed.

Double staining of tumor blood vessels (using anti-CD31 or PECAM) with CD8 showed that $CD8^+$ cells could be found outside blood vessels and within the tumor itself (Figs. 2B to E). Thus, some $CD8^+$ T cells appear to be able to undergo diapedesis through tumor-associated blood vessels to penetrate the tumor matrix.

$CD8^+$ T cells in mesothelioma tumors are activated

The tumor microenvironment was also assessed for signs of local antigen presentation (from the same animal shown in Figures 1B-E) after adoptive transfer of CFSE-labeled OT-1 cells. Very few OT-1 cells had penetrated the tumors 3 days after transfer however, those that had appeared to have proliferated (Figure 3B) as, unlike the same OT-I cells

transferred into mice given OVA in IFA (Figure 3A), there were no remaining parental cells. However, we could not exclude the possibility that they represent cells that proliferated elsewhere and then migrated into the tumor. Similarly, the tumor microenvironment was assessed for signs of local CTL activity from the same mice used for Figures 1E-J. Whilst there was clear CTL activity in the dLN (Figure 3C), the few target cells that could be detected in the tumor microenvironment showed no sign of loss of OVAp-pulsed target cells (Figure 3D) suggesting that intratumoral CTL had lost the killing ability they acquired in the dLN .

The activation status of MM-infiltrating $CD8^+$ T cells was also assessed using a range of markers including the early activation marker CD69 (Figure 3E), IFNγ (Figures 3F and G) and the peripheral LN homing marker, CD62L (data not shown), CD25 (Figure 3H) and the late activation marker, CD44 (Figure 3I) As expected, CD62L was downregulated on tumor-infiltrating $CD8^+$ T cells relative to those from LN. All other markers were upregulated on $CD8^+$ T cells in small MM tumors relative to their expression on $CD8^+$ T cells in normal LN or in tumor-draining LN. In particular, CD25 and CD44 were highly co-expressed by tumor-infiltrating $CD8^+$ T cells. $CD8^+$ T cells in tumor-dLN expressed higher levels of CD25, but not CD44, than their healthy counterparts (Figures 3H and I).

Tumor-specific $CD8^+$ T cells accumulate in MM tumors

The MHC class I SIINFEKL tetramer was used to identify endogenous tumor-specific $CD8^+$ T cells. $Tetramer^+CD8^+$ T cells were detected in low proportions (<1.6% of total CD8 population) in dLN throughout tumor growth (Figures 4B and C). In contrast, much higher levels (up to 15.7% of $CD8^+$ T cells were $tetramer^+$) were seen in MM tumors (Figures 4E and F). These $tetramer^+$ cells were activated, as shown by CD44 and CD69 expression (Figures 4G-I). Taken together, these data clearly show that, after tumor antigen is presented to naïve T cells in dLN, fully functional tumor-specific CTL are generated which home to the tumor. However, once in the tumor site their effector function appears compromised.

Activated $CD4^+$ T cells are also located in the MM tumor microenvironment

The presence of activated $CD8^+$ T cells within MM tumors does not provide much benefit to the host as the disease continues to progress implying local immunosuppression. One

suppressive cell type that has been recently identified is the $CD4^+$ regulatory T cell. Thus, we examined $CD4^+$ T cells in MM tumors versus those in tumor-draining and non-draining LN, and healthy LN. LN taken from MM-bearing hosts, regardless of tumor burden, contained significantly more $CD4^+$ T cells (27.9 ± 1.0% to 30.4 ± 1.3%) than normal LN (20.6 ± 0.7%; Figure 5A). However, the ratio of CD8:CD4 in tumor-dLN was 1.23:1; thus $CD8^+$ T cells outnumbered $CD4^+$ T cells. $CD4^+$ cells also infiltrated MM tumors in small numbers. The percentage of $CD4^+$ cells (ranging from 4.7 to 6.2%) within tumors did not change in with tumor burden and a ratio of 1:1 of CD8:CD4 was seen in the tumor bed. Similar to $CD8^+$ T cells, MM-infiltrating $CD4^+$ T cells were also activated as they expressed CD69, CD44 and secreted IFNγ (Figures 5B-I).

Expression of the α-chain of IL-2R (CD25) was also examined on $CD4^+$ T cells in MM-bearing hosts. CD25 expression can be indicative of activation however, CD25 co-expression with the nuclear transcription factor molecule, FoxP3, is recognised to be a marker of Treg cells. CD25 expression levels were not increased on $CD4^+$ T cells in MM-draining LN relative to healthy controls (Figure 5J). In contrast, increased expression levels of CD25 was seen on MM-infiltrating $CD4^+$ T cells (> 20% of $CD4^+$ cells).

$CD4^+$ cells are more likely to function as effector and not suppressor cells

Depletion studies were conducted to identify the function $CD4^+$ T cells exert on progressing tumors. As the depleting antibodies are rat antibodies they could only be used for two weeks before destruction by an anti-rat immune response. Transient removal of $CD4^+$ T cells did not have any impact upon tumor growth rate (Figure 6A). Use of mice that never have a mature $CD4^+$ T cell compartment (GK mice) resulted in a faster tumor growth rate that was significantly different to that seen in immunologically intact wild-type mice (Figure 6B), suggestive of a CD4 effector, and not regulator, phenotype. Thus, global removal of $CD4^+$ cells appears to remove an effector cell.

Splenic Treg cells do not ablate protective responses

The spleens of tumor-bearing mice may contain Tregs cells. Thus, to gain insights into their role, splenocytes prepared from healthy mice or from tumor-bearing mice were transferred into recipient mice which were then challenged with AE17 tumor cells 3 weeks later.

Recipients of splenocytes from tumor-bearing mice were completely protected (Figure 6C), whilst those from unburdened healthy mice were unable to prevent tumor growth. These data show that endogenously-generated, tumor antigen-specific splenic T cells provide significant levels of protection when transferred into a naïve host, and that co-located suppressor cells do not interfere with this process. Yet the same cells cannot protect the host within which they were induced, as their tumors continued to progress. These data suggest that there is site-specific regulatory activity within the tumor bed.

MM-infiltrating $CD4^+$ T regulatory (Treg) cells do not exert potent suppressor activity

Analysis of FoxP3 expression on $CD4^+$ T cells (independent of CD25), revealed putative Treg cells within the MM microenvironment (> 18%) (Figure 6D). There was no proportional increase of $FoxP3^+CD4^+$ T cells in tumor-draining LN relative to normal LN.

Treg cell depletion does not abrogate suppression of anti-MM immune responses

The above data suggested that the site of suppressive Treg function may be the tumor microenvironment. Therefore we wanted to deplete Treg cells in situ using an anti-CD25 monoclonal antibody (PC61), as depletion of $CD4^+$ Tregs by this antibody had been reported in several murine cancer models (36, 37) including MM (18, 34). FACS analysis showed that a single intra-tumoral injection of PC61 not only removed $CD4^+CD25^+FoxP3^+$ cells from the tumor microenvironment (Figures 7A-D) but also from all organs examined including LN, spleen (Figures 7E-L) and bone marrow for > 12 days (Figure 7M). Note also that less than 30% of tumor infiltrating $CD4^+CD25^+$ cells were $FoxP3^+$ (7C) suggesting that the remaining $CD4^+CD25^+$ cells may be activated effector cells; these cells were also depleted. Despite the global removal of $CD4^+CD25^+$ cells, MM tumors continued to progress at exactly the same rate as undepleted controls (Figure 7N).

Treg cell depletion does not improve immunotherapy

We have previously shown that intratumoral IL-2 immunotherapy is effective at curing small MM tumors (23) and hypothesized that depletion of Tregs may remove a population of cells that function as an IL-2 sink on account of their CD25 expression levels. Thus, removal of Tregs should improve effector cell responses. Instead, in vivo depletion of $CD25^+$ using PC61 completely disarmed IL-2 mediated effector function (Figure 8A). As

we have previously shown that IL-2 driven anti-tumor immunity is T cell mediated (23) we conclude that we removed effector and not regulator cells.

We also tested the role of Tregs when faced with IL-21 driven anti-tumor immunity. In this case, the removal of $CD25^{+}$ cells was a null event with no evidence of interference with effector or regulator cells (Figure 8B). Taken together, these data suggest either a weak role for Tregs as an anti-tumoral weapons, and/or that attempting their removal via CD25 targeting removes effectors as well as regulators.

Discussion

Mesothelioma tumors in patients and murine models alike are responsive to immune-enhancing agents delivered without a tumor antigen (3, 4, 6, 7, 20, 21, 23, 26, 27). These data suggest that as MM tumors evolve they engage with the adaptive immune system but that this immune response is insufficient and cannot prevent tumor growth without further help. Thus, we aimed to identify the point/s of immune failure using a unique MM model that secretes a soluble tumor antigen. We examined the main components of the anti-MM immune response, and focussed on the developing MM tumor microenvironment and sentinel LNs.

We clearly showed that developing MM tumors engage intimately with the immune response as the tumor antigen was rapidly presented to naïve T cells in LN resulting in the induction of CTLs. We speculated, but did not prove, that the cell type responsible for CTL induction was a cross-presenting DC (38-40). Interestingly, there was a proportional increase of DC in LNs as tumors progressed, and antigen presentation was so effective that the endogenous tumor-specific CTL generated were potent killers, indicating the activated status of these DC.

In an attempt to identify the location of the point of immune failure splenocytes were adoptively transferred from MM-bearing mice into healthy mice. The splenocytes provided powerful protection against tumor challenge confirming the potency of the systemic immune response induced against the tumor, and demonstrating that effector cells are located in the spleen. There was no evidence of splenic regulators however, the fate of transferred regulatory cells is unknown, they may require survival factors that are lacking in a healthy mouse or they may have trafficked to a different site. Nonetheless, taken together, these data show that the immune system is functional in secondary lymphoid organs and that this is not likely to be the site of immune failure in this model.

Note, our model is different to another MM model (AB1-HA) for which a weak CTL response is generated in, and restricted to, draining LN (41); thus, a point of immune failure in that model is also in the LN. One possible explanation to account for these differences may be that AB-1 expresses a membrane-bound marker antigen whilst our model secretes

its tumor antigen. A secreted tumor antigen is likely to be transported in a cell-independent manner to many LN and the spleen for uptake by resident DC which, in contrast to tumor-infiltrating DC, may not be subjected to tumor-associated suppression (42-44). As a result, CTL are generated systemically and have a greater chance of accessing the tumor site.

Human tumors contain infiltrating T cells, some of which may be tumor-specific (45-47) and tumor cells employ multiple immune-evading strategies. These data suggest that in humans tumor-specific T cells can leave the LN and penetrate the tumor microenvironment where they are restrained by powerful regulatory mechanisms. Thus, a significant point of immune failure for many cancers must be the tumor milieu. Examination of the MM microenvironment showed that despite elevated numbers of $CD8^+$ T cells in LN only small numbers of endogenous $CD8^+$ cells could be seen travelling in tumor-associated vasculature and inside the tumor itself. These data suggest that MM tumors may frustrate $CD8^+$ T cell penetrance. Nonetheless, increasing numbers of tumour-specific $CD8^+$ T cells emigrated into progressing tumors and were locally activated but functionally incapacitated, and MM tumors continued to progress suggesting local suppression. Therefore, we turned our attention to Tregs as they have been implicated as powerful local regulators in a number of animal models and in human studies (48). Small numbers of activated $CD4^+$ T cells were co-located in MM tumors of which less than 30% were $CD25^+FoxP3^+$. Thus, a substantial number may represent activated $CD4^+CD25^+$ T cells.

In vivo depletion of Tregs, often achieved by targeting CD25, can significantly improve anti-tumor immunity (49-53). However, there has been considerable debate about the effectiveness of this strategy (54) and others have reported incomplete depletion (55, 56) or unremarkable efficacies (36, 57, 58). In our hands, CD25-targeted Treg depletion did not modify tumor growth rate despite long term ablation of $CD4^+CD25^+$ cells throughout the body including bone marrow and secondary lymphoid organs. These data contrast to other studies of MM wherein CD25 depletion enabled effector cells to slow tumor progression (18, 34, 59). However, in those studies the anti-CD25 antibody was administered early; i.e. prior to tumor cell inoculation (18, 59), or when tumors were very small (34). We used established tumors that were greater than $20mm^2$ and found no meaningful benefit after CD25 depletion. Similarly, temporal removal of $CD4^+$ cells did not alter tumour growth

and their permanent absence adversely affected tumor development confirming their long-term effector role.

Finally, combining CD25-focused Treg depletion with cytokine-based immunotherapies either removed a $CD25^+$ effector population or represented a null event. The use of a depleting antibody that targets the alpha-chain of the IL-2 receptor may remove other populations likely to respond to IL-2 including $CD25^+CD4^+$ and $CD25^+CD8^+$ effector T cells and therefore contribute to the loss of effector function seen with IL-2 treatment. Indeed, we have preliminary data showing a reduction of activated $CD25^+CD8^+$ T cell numbers in lymphoid organs for greater than 12 days after use of PC61 (data not shown). In our IL-2 studies, the anti-CD25 injection occurred immediately before commencing IL-2 treatment. Thus, whilst Treg numbers remain low for 10-12 days, activated $CD4^+$ and $CD8^+$ T cell are also likely to have been ablated at the very time that requires their effector responses to IL-2.

These data differ to other reports as Treg depletion using anti-CD25 antibody has been shown to promote IL-2 driven tumor-infiltrating $CD8^+$ T cells and/or NK cells to eradicate tumors (60). Treg depletion has also been shown to improve IL-21-based anti-tumor immunotherapy (61). Overall, regardless of the model used, therapeutic $CD4^+CD25^+$ Treg cell depletion has failed to consistently enhance immune-based therapies (62). In contrast, prophylactic depletion, or depletion at the very early stages of tumor development appears to be more consistent and coincides with improved systemic anti-tumor responses (18, 34, 36, 51, 58, 59, 62). Taken together, these data suggest that Tregs may play an important role at the very early stages of tumor evolution, but once the tumor is established other regulatory mechanisms take over. Furthermore, targeting CD25 to remove Treg is fraught and unintended depletion of an important effector may occur.

The role of Treg cells remains contentious and may vary among different tumors. In humans, the prognostic influence of Treg in different cancers varies (63-66). Studies in MM patients' blood (67) or pleural effusions (68) did not find significant levels of $CD25^+FoxP3^+$ Treg cells relative to other cancers or healthy controls. There are also reports demonstrating a lack of correlation between cancer stage and the number or the function of peripheral Treg cells suggesting that these cells are not involved in tumor spreading (68).

Human MM tumors are reported to contain high levels of $Foxp3^+CD4^+CD25^+$ regulatory T-cells (18) and MM patients presenting with high levels of $CD4^+$ or $CD25^+$ tumor-infiltrating lymphocytes may have a trend toward shorter survival however, the presence of $FoxP3^+$ tumor-infiltrating lymphocytes did not affect survival (17).

Here, we show that the microenvironment of a MM murine model comprises of stromal elements, including activated immune cells. The presence of activated immune cells implies chronic inflammation, but despite this the tumor continues to grow. This may reflect events that occur in spontaneously arising tumors wherein products of oncogenes activated early in tumor development induce inflammatory responses and recruit immune cells into the tumor microenvironment (69). As a result, the evolving tumor and the immune system become intimately interconnected as tumor antigens are rapidly transported to draining LN wherein tumor-specific T cell responses are generated. Some of these T cells traffic into MM tumors where they appear phenotypically activated yet functionally incapable. However, the mechanism of this incapacitation does not appear to be substantially mediated by $CD25^+CD4^+$ Treg cells once MM tumors are established, and other more powerful, local suppressive factors are operating. The likely candidate for such suppression are the cytokines elaborated by tumor cells and by tumor-associated macrophages (18). Thus, it is unlikely that therapies directed at Treg cells will substantially improve anti-MM immunotherapy, particularly those that target the CD25 receptor as it risks removing a $CD25^+$ effector cell. Rather, therapies directed at augmenting or mimicking anti-tumor CD4 responses could be required which need to be directed at the tumor microenvironment for maximal effect.

ACKNOWLEDGMENTS

We thank the Centre for Microscopy, Characterisation and Analysis (CMCA) for help with the FACScan, as well as the staff at UWA animal holding areas in QEII hospital. The authors would also like to thank the National Health and Medical Research Council (NH&MRC), and the Western Australian Cancer Council for their funding contributions to these studies.

References

1. Berry, G., A. W. Musk, N. H. De Klerk, A. Johnson, and D. H. Yates. 2003. Predictions of mortality from mesothelioma. *Occup Environ Med 60:458*.
2. Robinson, B. W., C. Robinson, and R. A. Lake. 2001. Localised spontaneous regression in mesothelioma - possible immunological mechanism. *Lung Cancer 32:197-201*.
3. Robinson, B. W., S. A. Mukherjee, A. Davidson, S. Morey, A. W. Musk, I. Ramshaw, D. Smith, R. Lake, T. Haenel, M. Garlepp, J. Marley, C. Leong, I. Caminschi, and B. Scott. 1998. Cytokine gene therapy or infusion as treatment for solid human cancer. *J Immunother (1997) 21:211-217*.
4. Sterman, D. H., A. Recio, R. G. Carroll, C. T. Gillespie, A. Haas, A. Vachani, V. Kapoor, J. Sun, R. Hodinka, J. L. Brown, M. J. Corbley, M. Parr, M. Ho, I. Pastan, M. Machuzak, W. Benedict, X. Q. Zhang, E. M. Lord, L. A. Litzky, D. F. Heitjan, C. H. June, L. R. Kaiser, R. H. Vonderheide, S. M. Albelda, and M. Kanther. 2007. A phase I clinical trial of single-dose intrapleural IFN-beta gene transfer for malignant pleural mesothelioma and metastatic pleural effusions: high rate of antitumor immune responses. *Clin Cancer Res 13:4456-4466*.
5. Vachani, A., D. H. Sterman, and S. M. Albelda. 2007. Cytokine gene therapy for malignant pleural mesothelioma. *J Thorac Oncol 2:265-267*.
6. Christmas, T. I., L. S. Manning, M. J. Garlepp, A. W. Musk, and B. W. Robinson. 1993. Effect of interferon-alpha 2a on malignant mesothelioma. *J Interferon Res 13:9-12*.
7. Davidson, J. A., A. W. Musk, B. R. Wood, S. Morey, M. Ilton, L. L. Yu, P. Drury, K. Shilkin, and B. W. Robinson. 1998. Intralesional cytokine therapy in cancer: a pilot study of GM-CSF infusion in mesothelioma. *J Immunother (1997) 21:389-398*.
8. Belldegrun, A., L. M. Muul, and S. A. Rosenberg. 1988. Interleukin 2 expanded tumor-infiltrating lymphocytes in human renal cell cancer: isolation, characterization, and antitumor activity. *Cancer Res 48:206-214*.
9. Bukowski, R. M., W. Sharfman, S. Murthy, P. Rayman, R. Tubbs, J. Alexander, G. T. Budd, J. S. Sergi, L. Bauer, V. Gibson, and et al. 1991. Clinical results and

characterization of tumor-infiltrating lymphocytes with or without recombinant interleukin 2 in human metastatic renal cell carcinoma. *Cancer Res 51:4199-4205*.

10. Yannelli, J. R., E. Hirscowitz, and J. M. Wroblewski. 2003. Growth and functional reactivity of lymphocytes obtained from three anatomic compartments in patients with non-small-cell lung cancer (NSCLC). *Cancer Biother Radiopharm 18:735-749*.
11. McKee, M. D., A. Fichera, and M. I. Nishimura. 2007. T cell immunotherapy. *Front Biosci 12:919-932*.
12. Robinson, B. W., B. M. Scott, R. A. Lake, P. A. Stumbles, D. J. Nelson, S. Fisher, and A. L. Marzo. 2001. Lack of ignorance to tumor antigens: evaluation using nominal antigen transfection and T-cell receptor transgenic lymphocytes in Lyons-Parish analysis--implications for tumor tolerance. *Clin Cancer Res 7:811s-817s*.
13. Marzo, A. L., R. A. Lake, D. Lo, L. Sherman, A. McWilliam, D. Nelson, B. W. Robinson, and B. Scott. 1999. Tumor antigens are constitutively presented in the draining lymph nodes. *J Immunol 162:5838-5845*.
14. Gajewski, T. F., Y. Meng, C. Blank, I. Brown, A. Kacha, J. Kline, and H. Harlin. 2006. Immune resistance orchestrated by the tumor microenvironment. *Immunol Rev 213:131-145*.
15. Whiteside, T. L. 1998. Immune cells in the tumor microenvironment. Mechanisms responsible for functional and signaling defects. *Adv Exp Med Biol 451:167-171*.
16. Mudhar, H. S., P. M. Fisher, and W. A. Wallace. 2002. No relationship between tumour infiltrating lymphocytes and overall survival is seen in malignant mesothelioma of the pleura. *Eur J Surg Oncol 28:564-565*.
17. Anraku, M., K. S. Cunningham, Z. Yun, M. S. Tsao, L. Zhang, S. Keshavjee, M. R. Johnston, and M. de Perrot. 2008. Impact of tumor-infiltrating T cells on survival in patients with malignant pleural mesothelioma. *J Thorac Cardiovasc Surg 135:823-829*.
18. Hegmans, J. P., A. Hemmes, H. Hammad, L. Boon, H. C. Hoogsteden, and B. N. Lambrecht. 2006. Mesothelioma environment comprises cytokines and T-regulatory cells that suppress immune responses. *Eur Respir J 27:1086-1095*.
19. Jarnicki, A. G., D. R. Fitzpatrick, B. W. Robinson, and H. Bielefeldt-Ohmann. 1996. Altered CD3 chain and cytokine gene expression in tumor infiltrating T lymphocytes during the development of mesothelioma. *Cancer Lett 103:1-9*.

20. Caminschi, I., E. Venetsanakos, C. C. Leong, M. J. Garlepp, B. Scott, and B. W. Robinson. 1998. Interleukin-12 induces an effective antitumor response in malignant mesothelioma. *Am J Respir Cell Mol Biol 19:738-746*.

21. Cordier Kellerman, L., L. Valeyrie, N. Fernandez, P. Opolon, J. C. Sabourin, E. Maubec, P. Le Roy, A. Kane, A. Legrand, M. A. Abina, V. Descamps, and H. Haddada. 2003. Regression of AK7 malignant mesothelioma established in immunocompetent mice following intratumoral gene transfer of interferon gamma. *Cancer Gene Ther 10:481-490*.

22. Friedlander, P. L., C. L. Delaune, J. M. Abadie, M. Toups, J. LaCour, L. Marrero, Q. Zhong, and J. K. Kolls. 2003. Efficacy of CD40 ligand gene therapy in malignant mesothelioma. *Am J Respir Cell Mol Biol 29:321-330*.

23. Jackaman, C., C. S. Bundell, B. F. Kinnear, A. M. Smith, P. Filion, D. van Hagen, B. W. Robinson, and D. J. Nelson. 2003. IL-2 intratumoral immunotherapy enhances CD8+ T cells that mediate destruction of tumor cells and tumor-associated vasculature: a novel mechanism for IL-2. *J Immunol 171:5051-5063*.

24. Astoul, P., D. Picat-Joossen, J. R. Viallat, and C. Boutin. 1998. Intrapleural administration of interleukin-2 for the treatment of patients with malignant pleural mesothelioma: a Phase II study. *Cancer 83:2099-2104*.

25. Boutin, C., J. R. Viallat, and P. Astoul. 1990. [Treatment of mesothelioma with interferon gamma and interleukin 2]. *Rev Pneumol Clin 46:211-215*.

26. Castagneto, B., S. Zai, L. Mutti, A. Lazzaro, R. Ridolfi, E. Piccolini, A. Ardizzoni, L. Fumagalli, G. Valsuani, and M. Botta. 2001. Palliative and therapeutic activity of IL-2 immunotherapy in unresectable malignant pleural mesothelioma with pleural effusion: Results of a phase II study on 31 consecutive patients. *Lung Cancer 31:303-310*.

27. Mukherjee, S., T. Haenel, R. Himbeck, B. Scott, I. Ramshaw, R. A. Lake, G. Harnett, P. Phillips, S. Morey, D. Smith, J. A. Davidson, A. W. Musk, and B. Robinson. 2000. Replication-restricted vaccinia as a cytokine gene therapy vector in cancer: persistent transgene expression despite antibody generation. *Cancer Gene Ther 7:663-670*.

28. Creaney, J., H. Christansen, R. Lake, A. B. Musk, N. de Klerk, and B. W. Robinson. 2006. Soluble mesothelin related protein in mesothelioma. *J Thorac Oncol 1:172-174*.

29. Creaney, J., D. Yeoman, L. K. Naumoff, M. Hof, A. Segal, A. W. Musk, N. De Klerk, N. Horick, S. J. Skates, and B. W. Robinson. 2007. Soluble mesothelin in effusions: a useful tool for the diagnosis of malignant mesothelioma. *Thorax 62:569-576*.

30. Hogquist, K. A., S. C. Jameson, W. R. Heath, J. L. Howard, M. J. Bevan, and F. R. Carbone. 1994. T cell receptor antagonist peptides induce positive selection. *Cell 76:17-27*.

31. Zhan, Y., A. J. Corbett, J. L. Brady, R. M. Sutherland, and A. M. Lew. 2000. Delayed rejection of fetal pig pancreas in CD4 cell deficient mice was correlated with residual helper activity. *Xenotransplantation 7:267-274*.

32. Kagi, D., B. Ledermann, K. Burki, P. Seiler, B. Odermatt, K. J. Olsen, E. R. Podack, R. M. Zinkernagel, and H. Hengartner. 1994. Cytotoxicity mediated by T cells and natural killer cells is greatly impaired in perforin-deficient mice. *Nature 369:31-37*.

33. Lyons, A. B., and C. R. Parish. 1994. Determination of lymphocyte division by flow cytometry. *J Immunol Methods 171:131-137*.

34. Needham, D. J., J. X. Lee, and M. W. Beilharz. 2006. Intra-tumoural regulatory T cells: a potential new target in cancer immunotherapy. *Biochem Biophys Res Commun 343:684-691*.

35. Suda, T., and D. Liu. 2007. Hydrodynamic gene delivery: its principles and applications. *Mol Ther 15:2063-2069*.

36. Tanaka, H., J. Tanaka, J. Kjaergaard, and S. Shu. 2002. Depletion of CD4+ CD25+ regulatory cells augments the generation of specific immune T cells in tumor-draining lymph nodes. *J Immunother 25:207-217*.

37. Haeryfar, S. M., R. J. DiPaolo, D. C. Tscharke, J. R. Bennink, and J. W. Yewdell. 2005. Regulatory T cells suppress CD8+ T cell responses induced by direct priming and cross-priming and moderate immunodominance disparities. *J Immunol 174:3344-3351*.

38. Sotomayor, E. M., I. Borrello, F. M. Rattis, A. G. Cuenca, J. Abrams, K. Staveley-O'Carroll, and H. I. Levitsky. 2001. Cross-presentation of tumor antigens by bone marrow-derived antigen-presenting cells is the dominant mechanism in the induction of T-cell tolerance during B-cell lymphoma progression. *Blood 98:1070-1077*.

39. van Mierlo, G. J., Z. F. Boonman, H. M. Dumortier, A. T. den Boer, M. F. Fransen, J. Nouta, E. I. van der Voort, R. Offringa, R. E. Toes, and C. J. Melief. 2004. Activation of dendritic cells that cross-present tumor-derived antigen licenses CD8+ CTL to cause tumor eradication. *J Immunol 173:6753-6759*.

40. Nelson, D. J., S. Mukherjee, C. Bundell, S. Fisher, D. van Hagen, and B. Robinson. 2001. Tumor progression despite efficient tumor antigen cross-presentation and effective "arming" of tumor antigen-specific CTL. *J Immunol 166:5557-5566*.

41. Stumbles, P. A., R. Himbeck, J. A. Frelinger, E. J. Collins, R. A. Lake, and B. W. Robinson. 2004. Cutting edge: tumor-specific CTL are constitutively cross-armed in draining lymph nodes and transiently disseminate to mediate tumor regression following systemic CD40 activation. *J Immunol 173:5923-5928*.

42. Zeng, Z., X. Xu, Y. Zhang, J. Xing, J. Long, L. Gu, X. Wang, D. Sun, W. Ka, W. Yao, Z. Wen, and S. Chien. 2007. Tumor-derived factors impaired motility and immune functions of dendritic cells through derangement of biophysical characteristics and reorganization of cytoskeleton. *Cell Motil Cytoskeleton 64:186-198*.

43. Sharma, S., M. Stolina, S. C. Yang, F. Baratelli, J. F. Lin, K. Atianzar, J. Luo, L. Zhu, Y. Lin, M. Huang, M. Dohadwala, R. K. Batra, and S. M. Dubinett. 2003. Tumor cyclooxygenase 2-dependent suppression of dendritic cell function. *Clin Cancer Res 9:961-968*.

44. Ohm, J. E., and D. P. Carbone. 2001. VEGF as a mediator of tumor-associated immunodeficiency. *Immunol Res 23:263-272*.

45. Shimabukuro, T., and K. Naito. 2008. Tumor-infiltrating lymphocytes derived from human renal cell carcinoma: clonal analysis of its characteristics. *Int J Urol 15:241-244*.

46. Itoh, K., C. D. Platsoucas, and C. M. Balch. 1988. Autologous tumor-specific cytotoxic T lymphocytes in the infiltrate of human metastatic melanomas. Activation by interleukin 2 and autologous tumor cells, and involvement of the T cell receptor. *J Exp Med 168:1419-1441*.

47. Piersma, S. J., M. J. Welters, J. M. van der Hulst, J. N. Kloth, K. M. Kwappenberg, B. J. Trimbos, C. J. Melief, B. W. Hellebrekers, G. J. Fleuren, G. G. Kenter, R. Offringa, and S. H. van der Burg. 2008. Human papilloma virus specific T cells

infiltrating cervical cancer and draining lymph nodes show remarkably frequent use of HLA-DQ and -DP as a restriction element. *Int J Cancer 122:486-494*.

48. Yamaguchi, T., and S. Sakaguchi. 2006. Regulatory T cells in immune surveillance and treatment of cancer. *Semin Cancer Biol 16:115-123*.
49. Heier, I., P. O. Hofgaard, P. Brandtzaeg, F. L. Jahnsen, and M. Karlsson. 2008. Depletion of CD4+ CD25+ regulatory T cells inhibits local tumour growth in a mouse model of B cell lymphoma. *Clin Exp Immunol 152:381-387*.
50. Chen, Y. L., J. H. Fang, M. D. Lai, and Y. S. Shan. 2008. Depletion of CD4(+)CD25(+) regulatory T cells can promote local immunity to suppress tumor growth in benzo[a]pyrene-induced forestomach carcinoma. *World J Gastroenterol 14:5797-5809*.
51. Johnson, B. D., W. Jing, and R. J. Orentas. 2007. CD25+ regulatory T cell inhibition enhances vaccine-induced immunity to neuroblastoma. *J Immunother 30:203-214*.
52. Matsushita, N., S. A. Pilon-Thomas, L. M. Martin, and A. I. Riker. 2008. Comparative methodologies of regulatory T cell depletion in a murine melanoma model. *J Immunol Methods 333:167-179*.
53. Ohmura, Y., K. Yoshikawa, S. Saga, R. Ueda, Y. Kazaoka, and S. Yamada. 2008. Combinations of tumor-specific CD8+ CTLs and anti-CD25 mAb provide improved immunotherapy. *Oncol Rep 19:1265-1270*.
54. Colombo, M. P., and S. Piconese. 2007. Regulatory-T-cell inhibition versus depletion: the right choice in cancer immunotherapy. *Nat Rev Cancer 7:880-887*.
55. Couper, K. N., D. G. Blount, J. B. de Souza, I. Suffia, Y. Belkaid, and E. M. Riley. 2007. Incomplete depletion and rapid regeneration of Foxp3+ regulatory T cells following anti-CD25 treatment in malaria-infected mice. *J Immunol 178:4136-4146*.
56. McNeill, A., E. Spittle, and B. T. Backstrom. 2007. Partial depletion of CD69low-expressing natural regulatory T cells with the anti-CD25 monoclonal antibody PC61. *Scand J Immunol 65:63-69*.
57. Degl'Innocenti, E., M. Grioni, G. Capuano, E. Jachetti, M. Freschi, M. T. Bertilaccio, R. Hess-Michelini, C. Doglioni, and M. Bellone. 2008. Peripheral T-cell tolerance associated with prostate cancer is independent from CD4+CD25+ regulatory T cells. *Cancer Res 68:292-300*.

58. Curtin, J. F., M. Candolfi, T. M. Fakhouri, C. Liu, A. Alden, M. Edwards, P. R. Lowenstein, and M. G. Castro. 2008. Treg depletion inhibits efficacy of cancer immunotherapy: implications for clinical trials. *PLoS ONE 3:e1983*.

59. Rudge, G., S. P. Barrett, B. Scott, and I. R. van Driel. 2007. Infiltration of a mesothelioma by IFN-gamma-producing cells and tumor rejection after depletion of regulatory T cells. *J Immunol 178:4089-4096*.

60. Imai, H., M. Saio, K. Nonaka, T. Suwa, N. Umemura, G. F. Ouyang, J. Nakagawa, H. Tomita, S. Osada, Y. Sugiyama, Y. Adachi, and T. Takami. 2007. Depletion of CD4+CD25+ regulatory T cells enhances interleukin-2-induced antitumor immunity in a mouse model of colon adenocarcinoma. *Cancer Sci 98:416-423*.

61. Comes, A., O. Rosso, A. M. Orengo, E. Di Carlo, C. Sorrentino, R. Meazza, T. Piazza, B. Valzasina, P. Nanni, M. P. Colombo, and S. Ferrini. 2006. CD25+ regulatory T cell depletion augments immunotherapy of micrometastases by an IL-21-secreting cellular vaccine. *J Immunol 176:1750-1758*.

62. Quezada, S. A., K. S. Peggs, T. R. Simpson, Y. Shen, D. R. Littman, and J. P. Allison. 2008. Limited tumor infiltration by activated T effector cells restricts the therapeutic activity of regulatory T cell depletion against established melanoma. *J Exp Med 205:2125-2138*.

63. Grabenbauer, G. G., G. Lahmer, L. Distel, and G. Niedobitek. 2006. Tumor-infiltrating cytotoxic T cells but not regulatory T cells predict outcome in anal squamous cell carcinoma. *Clin Cancer Res 12:3355-3360*.

64. Yoshioka, T., M. Miyamoto, Y. Cho, K. Ishikawa, T. Tsuchikawa, M. Kadoya, L. Li, R. Mishra, K. Ichinokawa, Y. Shoji, Y. Matsumura, T. Shichinohe, S. Hirano, T. Shinohara, T. Itoh, and S. Kondo. 2008. Infiltrating regulatory T cell numbers is not a factor to predict patient's survival in oesophageal squamous cell carcinoma. *Br J Cancer 98:1258-1263*.

65. Lee, N. R., E. K. Song, K. Y. Jang, H. N. Choi, W. S. Moon, K. Kwon, J. H. Lee, C. Y. Yim, and J. Y. Kwak. 2008. Prognostic impact of tumor infiltrating FOXP3 positive regulatory T cells in diffuse large B-cell lymphoma at diagnosis. *Leuk Lymphoma 49:247-256*.

66. Mizukami, Y., K. Kono, Y. Kawaguchi, H. Akaike, K. Kamimura, H. Sugai, and H. Fujii. 2008. Localisation pattern of Foxp3+ regulatory T cells is associated with clinical behaviour in gastric cancer. *Br J Cancer 98:148-153*.

67. Meloni, F., M. Morosini, N. Solari, I. Passadore, C. Nascimbene, M. Novo, M. Ferrari, M. Cosentino, F. Marino, E. Pozzi, and A. M. Fietta. 2006. Foxp3 expressing CD4+ CD25+ and CD8+CD28- T regulatory cells in the peripheral blood of patients with lung cancer and pleural mesothelioma. *Hum Immunol 67:1-12*.

68. DeLong, P., R. G. Carroll, A. C. Henry, T. Tanaka, S. Ahmad, M. S. Leibowitz, D. H. Sterman, C. H. June, S. M. Albelda, and R. H. Vonderheide. 2005. Regulatory T cells and cytokines in malignant pleural effusions secondary to mesothelioma and carcinoma. *Cancer Biol Ther 4:342-346*.

69. Finn, O. J. 2008. Cancer immunology. *N Engl J Med 358:2704-2715*.

Figure legends

Figure 1. DC presentation of MM-antigens to naïve T cells generates effector CTLs

Tumor and draining lymph nodes (dLN) single cell suspensions prepared from mice bearing small and medium tumors were stained with anti-CD11c for DCs. Pooled data (A) is from 2 experiments (6 mice/group) and represented as mean percentage of total cells ± SEM, * = $p<0.05$ comparing tumor-dLN to normal LN. To analyze MM-antigen presentation to naïve T cells CFSE-labelled, tumor antigen-specific, OT-I T cells were adoptively transferred into recipient AE17sOVA-bearing mice three days prior to analysis. The dLN (B) and non-dLNs (C) were harvested from recipient mice, prepared as a single cell suspension and stained for CD8. FACS analysis was performed by gating on $CD8^+/CFSE^+$ cells. Mice inoculated with AE17 tumor cells were negative controls (D and E). Representative histograms are shown (B-E). In vivo CTL activity was assessed by adoptively transferring differentially-labelled target cells prepared from normal mice representing $CFSE^{high}$ or OVAp (SIIN), and $CFSE^{low}$ control cells into mice bearing AE17-sOVA or AE17 tumors. Eighteen hours later, dLN and non-dLN were prepared as a single suspension and FACS analysed. A reduction in the SIIN peak compared to the control peak represents lysis of the targets. Representative histograms are shown (F-I). CTL activity is shown as the number of cells in the SIIN peak/number of cells in the control peak x 100. All data within each experiment was normalised compared to non-tumor bearing C57BL/6J LN controls. Pooled data (9 mice/group) from dLN and non-dLN (C) is shown as mean ± SEM. One way ANOVA was performed comparing small versus medium sized tumors; ** = $p<0.01$.

Figure 1

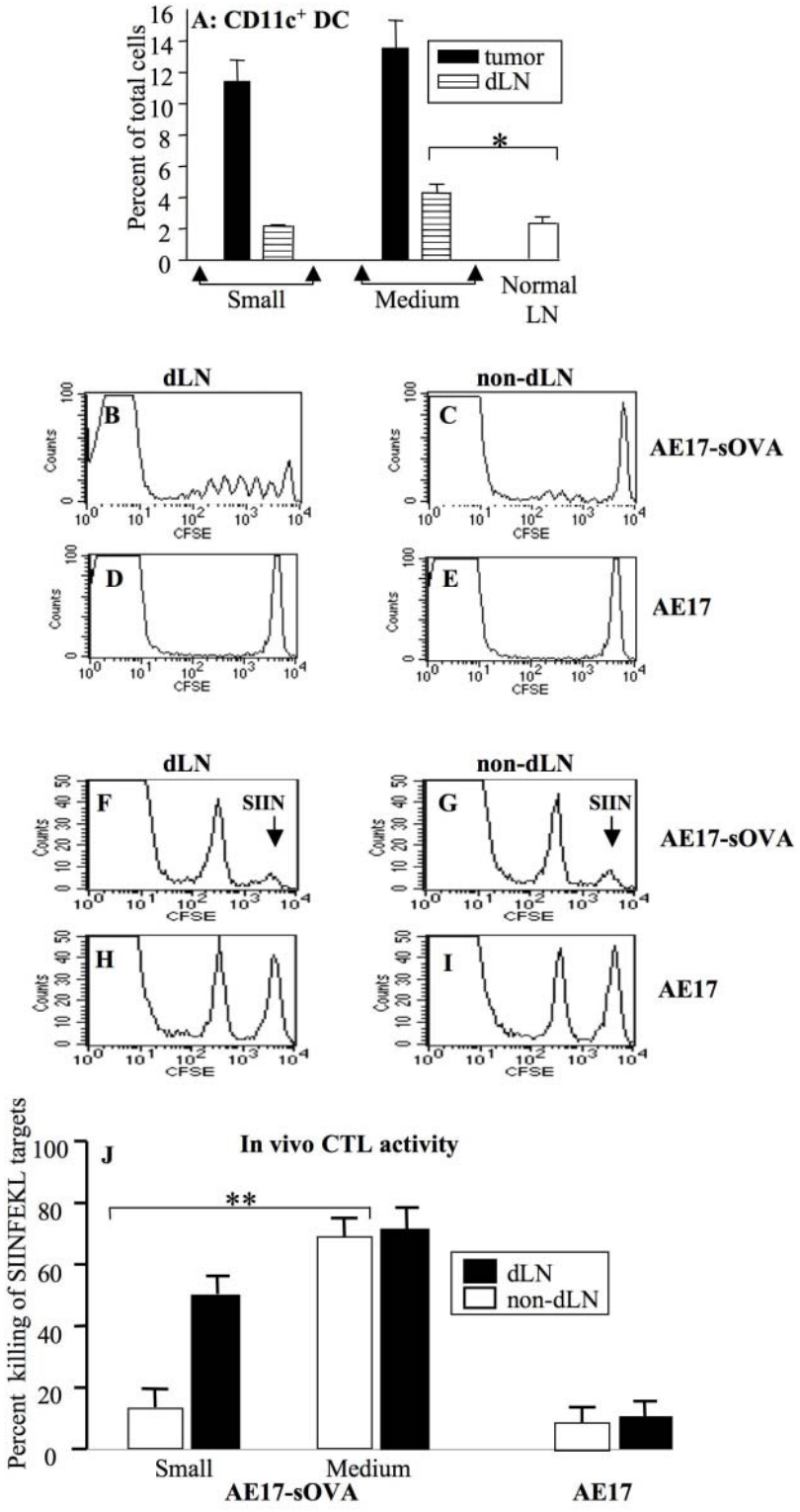

Figure 2. CD8$^+$ cells penetrate the MM tumor microenvironment

Similar to Figure 1, single cell suspension of small or medium tumors and their LN were stained for CD8 and pooled data from 3 experiments (9 mice/group) shown as the mean ± SEM (A) with *** = $p<0.001$ comparing dLN and non-dLN to normal LN. Frozen tumor sections were double stained for $CD8^+$ cells (blue; B, D and E) and CD31 to detect blood vessels (brown; C, D and E). Rat IgG2a (B) and rat IgG2b (C) are isotype controls. These experiments were performed twice (6 mice/group) and representative photos at 200x magnification are shown. The inset (E) shows a $CD8^+$ cell associated with a tumor blood vessel, and a $CD8^+$ cell within the tumor matrix, indicated by arrows.

Figure 2

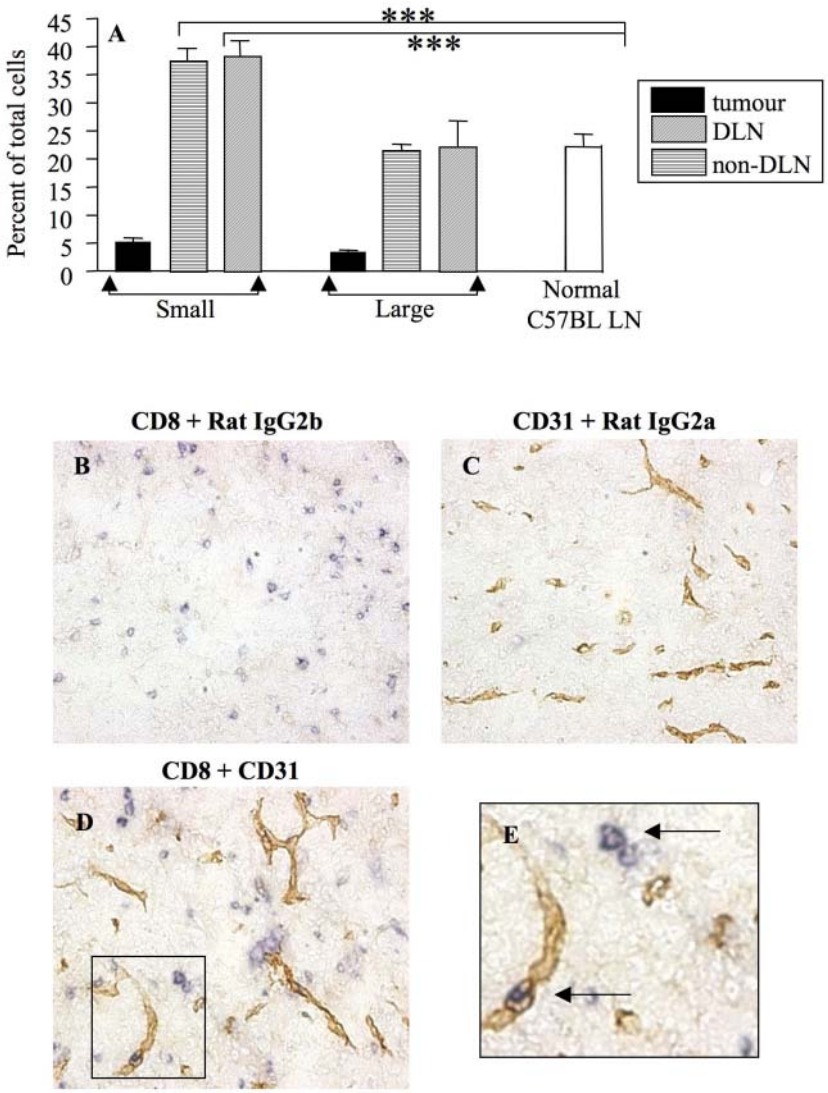

Figure 3. MM-infiltrating CD8$^+$ T cells are activated but lose CTL activity

Tumors were also harvested from AE17sOVA-bearing mice given CFSE-labelled, tumor antigen specific, OT-I T cells (as per Figures 1B and C). The few OT-I cells that penetrated the tumor expressed low levels of CFSE similar to proliferating cells seen in mice given OVA in Incomplete Freunds Adjuvant (OVA/IFA) dLN, indicative of proliferation (A). However, the few $CFSE^{high}$ (OVAp) and $CFSE^{low}$ target cells harvested from the tumors of AE17sOVA-bearing mice (as per Figures 1F and G) showed no in vivo CTL activity (D) relative to the CTL activity in dLN of the same mouse (C). In separate experiments, tumors and dLN harvested from AE17-bearing mice were double stained for CD8 and CD69 (E), IFNγ (F and G), CD25 (H) and CD44 (I). FACS analysis was performed by gating on $CD8^+$ cells. Representative histograms are shown with dLN and tumor overlaid for CD69 (E). For IFNγ analysis in the dLN (F) and tumor (G) the bold line represents IFNγ and the light line represents the rat IgG1 isotype control. These experiments were repeated twice (6 mice/group). Pooled data from 2 experiments (6 mice/group) is shown for CD25 (H) and CD44 (I) as mean percent of CD8 cells ± SEM. ** = $p<0.01$, comparing dLN and to normal LN.

Figure 3

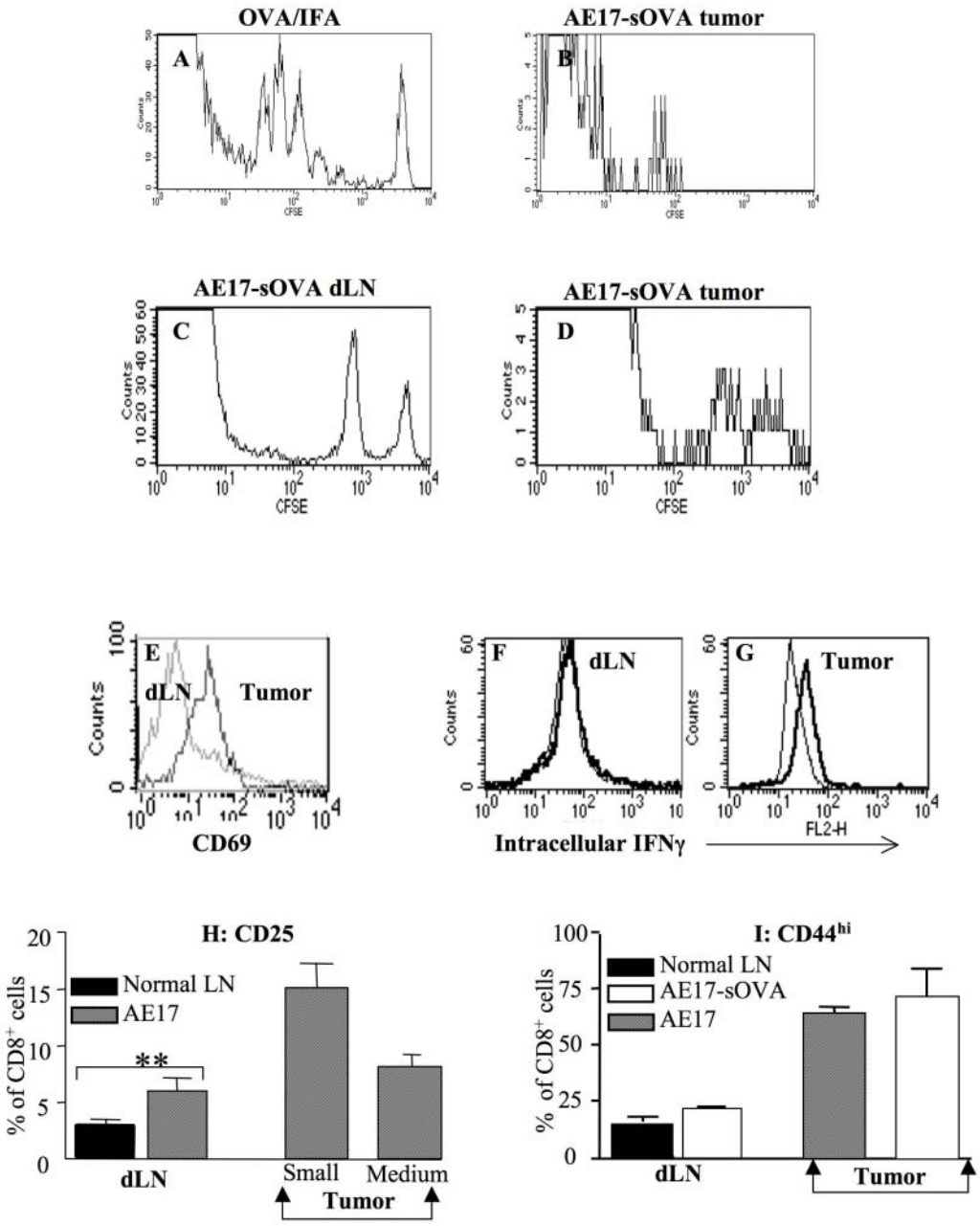

Figure 4. Tumor-specific $CD8^+$ cells in MM tumors are also activated

Draining LN (dLN; A and B) and tumors (D and E) and were harvested from AE17 (A and D) and AE17-sOVA (B and E) tumor-bearing mice and FACS analysed for co-expression of the SIINFEKL (OVAp) tetramer and CD8 (A-F), as well as an isotype control (G), CD44 (H) or CD69 (I). Flow cytometric analysis was performed by gating on $CD8^{+}tetramer^{+}$ cells. Representative dot plots (A, B, D and E) and histograms (G-I) are shown. Pooled data from 2 experiments (6 mice/group) is shown as mean percent of CD8 cells that are $tetramer^{+}$ ± SEM in the dLN (C) and tumor (F). *** = $p<0.001$ comparing small tumors to the larger tumors.

Figure 4

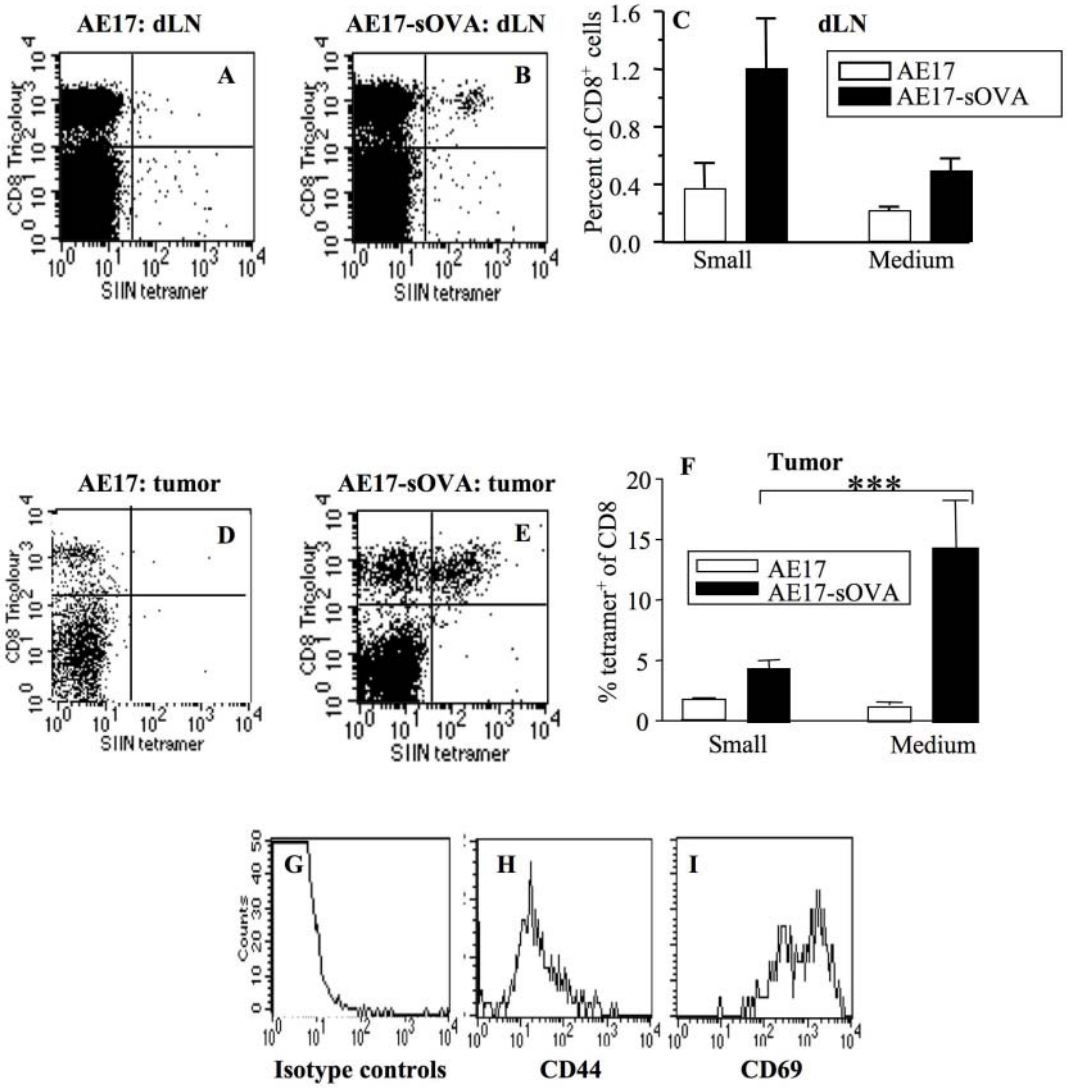

Figure 5. MM-infiltrating CD4$^+$ T cells are activated

Tumors and dLN were harvested from AE17-bearing mice and stained for CD4 expression and FACS analyzed. These experiments were repeated twice (6 mice/group) and pooled data is shown as mean percent of $CD4^+$ cells ± SEM (A). * = $p<0.05$ and** = $p<0.01$, comparing dLN and non-dLN to normal LN. Cells were also double stained for CD4 and isotype controls (B and F), CD69 (C and G), CD44 (D and H) as well as IFNγ (E and I). FACS analysis was performed by gating on $CD4^+$ cells and representative FACS histograms are shown (B-I). For IFNγ analysis (E and I), the bold line represents the IFNγ and the light line represents the isotype control. $CD4^+CD25^+$ co-expression was also examined in normal LN, dLN and tumors and pooled data from 2 experiments with (6 mice/group) is shown as the percent of $CD4^+$ that are $CD25^+$ ± SEM (J).

Figure 5

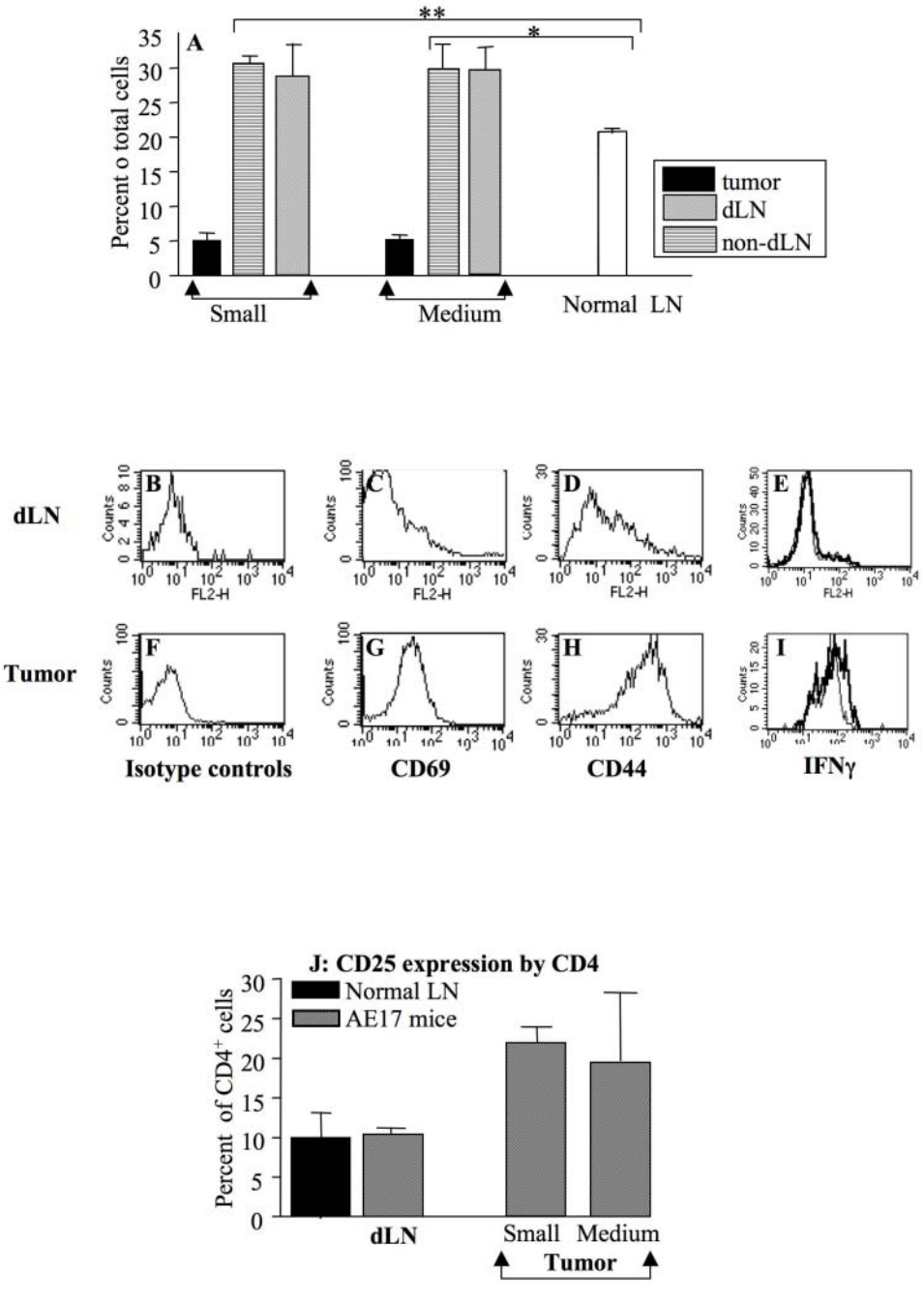

Figure 6. The majority of $CD4^+$ cells are effector cells

The role of $CD4^+$ cells was determined by antibody depletion (A), and by the use of GK mice (B); pooled data shown as mean tumor size ± SEM from 5 mice/group. Only GK mice were significantly different to C57BL/6 mice (B). To address a possible role for splenic cells, naïve C57BL/6 mice were the recipients of adoptively transferred, unfractionated spleen cells prepared from unmanipulated, healthy mice and from mice with progressing AE17 tumors (C). Three weeks later all mice, plus tumor growth controls (no transfer), were challenged with AE17 tumor cells. Pooled data from 1 of 2 experiments (8 mice/group) is shown as mean ± SEM (C). Tumor and dLN from AE17 tumor-bearing mice were FACS analysed for $CD4^+FoxP3^+$ co-expression in normal LN, tumor dLN and tumors (D); pooled data shown after gating on $CD4^+$ cells from 12 mice/group.

Figure 6

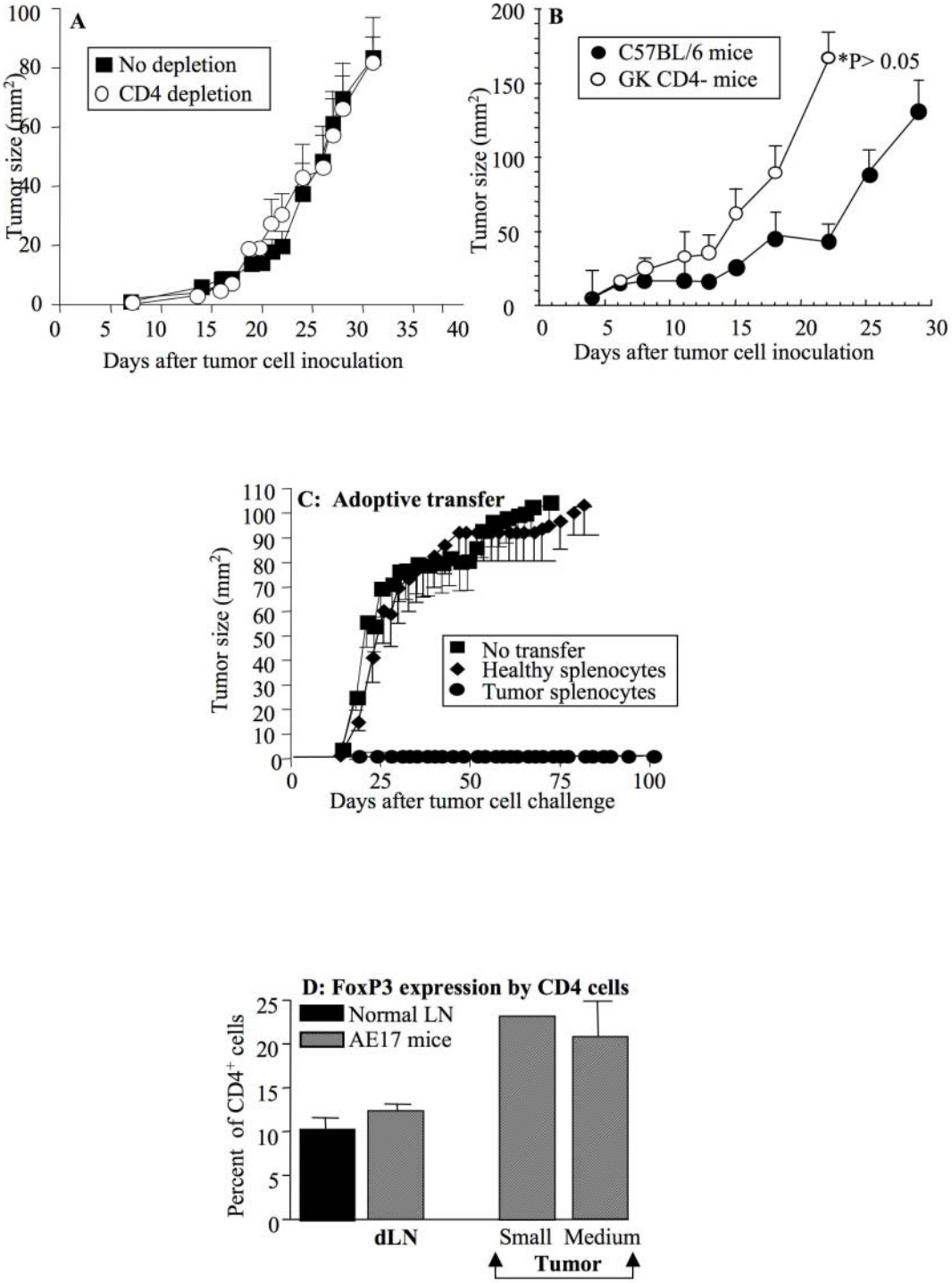

Figure 7. $CD25^{+}CD4^{+}$ Tregs do not interfere with endogenous anti-MM immunity

The role of $CD4^+CD25^+$ suppressor cells was determined by depletion using the anti-CD25 antibody (PC61). A single intra-tumoral injection of PC61 depleted $CD4^+CD25^+FoxP3^+$ from the tumor (A,-D), DLN (E-H), spleen (I-L) and bone marrow for 10 days (M). Representative dot plots 4 or 6 days after PC61 injection show $CD4^+CD25^+$ (A,B,E,F,I,J) gated on lymphocytes, and $FoxP3^+CD25^+$ gated on $CD4^+CD25^+$ (C,D,G,H,K,L). Data is from one of 3 experiments in which the organs from 5 mice/group were pooled for analysis. Mice were given one or two PC61 injections (arrows) and tumor growth monitored (3 experiments with 5 mice/group) (N); data shown as mean ± SEM.

Figure 7

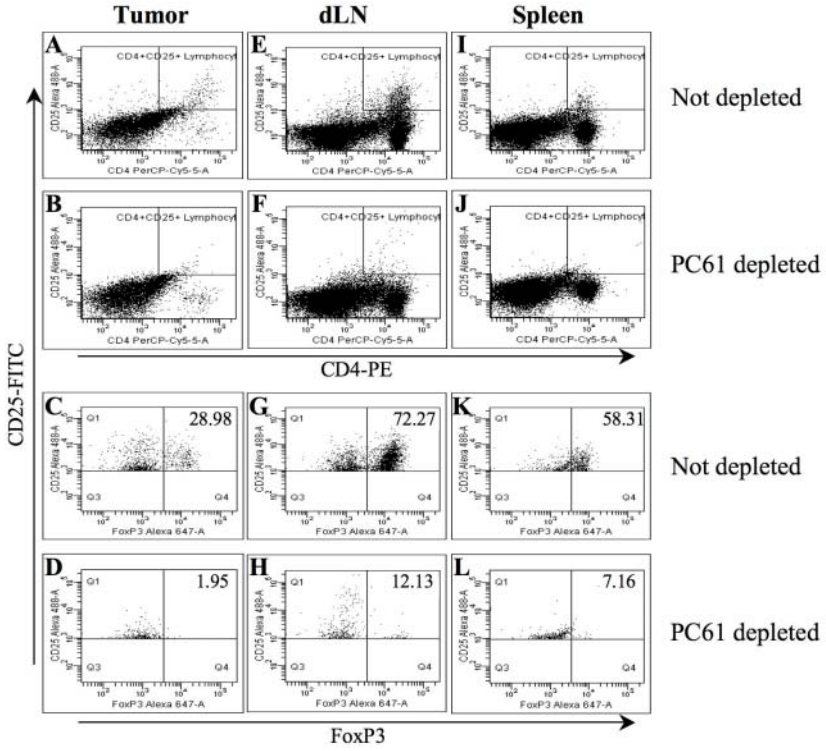
Tumor
dLN
Spleen
A
E
I
Not depleted
B
F
J
PC61 depleted
CD4-PE
CD25-FITC
C
G
K
28.98
72.27
58.31
Not depleted
D
H
L
1.95
12.13
7.16
PC61 depleted
FoxP3

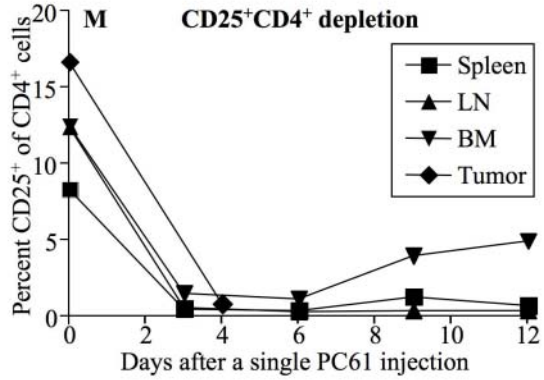
M
CD25+CD4+ depletion
Spleen
LN
BM
Tumor
Percent CD25+ of CD4+ cells
Days after a single PC61 injection

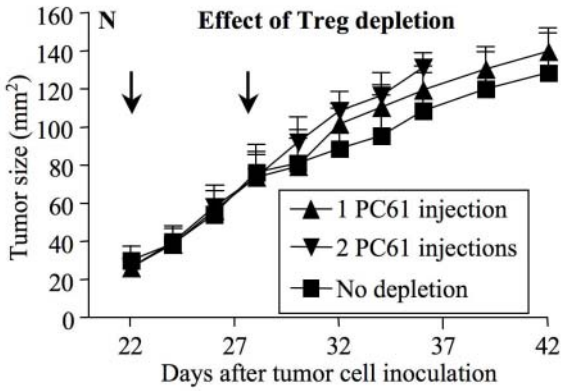
N
Effect of Treg depletion
1 PC61 injection
2 PC61 injections
No depletion
Tumor size (mm2)
Days after tumor cell inoculation

Figure 8. CD25-targeted Treg depletion may confound cytokine-based immunotherapy

A single PC61 injection was given one day prior to intratumoral IL-2 injections given every 2nd day (2 experiments with 5 mice/group). PC61 injections were given one day before each of 2 hydrodynamic injections of pORF.mIL-21 that were 6 days apart (1 experiment with 5 mice/group), and tumor growth monitored. Data shown as mean ± SEM.

Figure 8

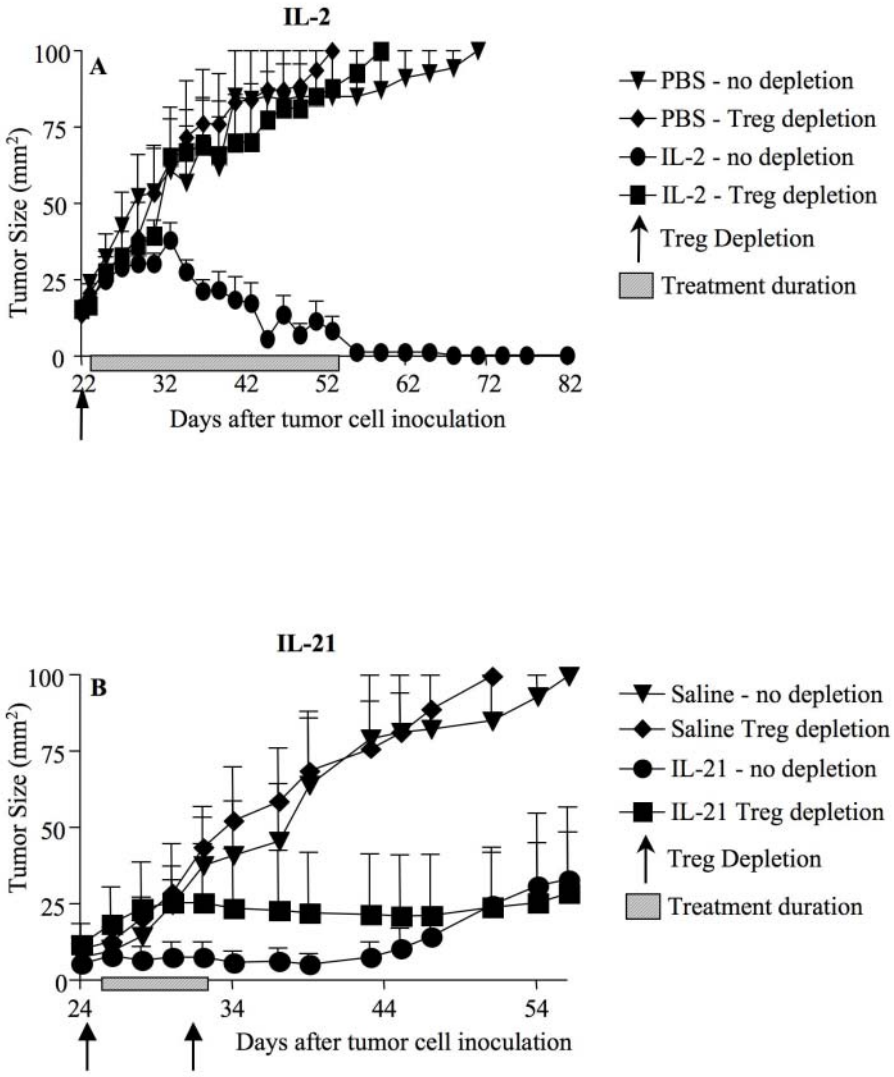
IL-2
A
Tumor Size (mm²)
100
75
50
25
0
22
32
42
52
62
72
82
Days after tumor cell inoculation
PBS - no depletion
PBS - Treg depletion
IL-2 - no depletion
IL-2 - Treg depletion
Treg Depletion
Treatment duration
IL-21
B
Tumor Size (mm²)
100
75
50
25
0
24
34
44
54
Days after tumor cell inoculation
Saline - no depletion
Saline Treg depletion
IL-21 - no depletion
IL-21 Treg depletion
Treg Depletion
Treatment duration